P9.74 MONITORING POLARIMETRIC WEATHER RADAR CALIBRATION

L. Borowska[(1)*], D. Zrnic[(1)]
(1) National Severe Storms Laboratory, USA

1. INTRODUCTION

Calibration of operational radars should be maintained continuously and be as automated as possible. To achieve precision in measurements of reflectivity on the WSR-88D, automatic calibration of the receiver is performed between volume scans. Transmitter power is measured at eight hour intervals (the frequency could be increased and it is in principle possible to monitor the stability of transmit-receive path from the existing sample of the transmitted pulse). The procedure does require built in signal generator and control circuits; hence on many types of radar it is not feasible.

An alternative monitoring of deviation in radar parameters affecting calibration was suggested by Rinehart (1978) who used peak cross sections of ground scatterers to check variations in Z. Sielberstein et al. (2008) computed daily cumulative distribution function of combined ground clutter and precipitation reflectivity irrespective whether precipitation was present or absent over the clutter area. In their data the values of reflectivity at the 95th percentile and higher were exclusively due to ground returns. Hence daily change in the 95th percentile was attributed to variation of sensitivity (failure of components, change in receiver gain, transmitted power, etc.). The baseline 95th percentile was set to 50 dBZ because it exceeded reflectivities of rain at Kwajalein where measurements were made.

Differential reflectivity needs accurate calibration to control bias in rainfall estimates and classification of precipitation; the rainfall estimator tested by Ryzhkov et al. (2005) has a bias error of 18 % if the bias of Z_{DR} is 0.2 dB. Therefore, smaller bias is desirable (value of 0.1 dB is specified for the WSR-88D network). Use of data for that purpose is preferred compared to intrusive measurement with power meters; hence few data based calibration methods have been devised. Among these the Z_{DR} calibration at vertical incidence is common. It entails observing precipitation at vertical incidence while the antenna rotates about its axis (Gorgucci et al. 1999; Bringi and Chandrasekar 2001). Precipitation particles have no preferential orientation in a horizontal plane therefore differential reflectivity should be zero. Departure from zero captures the overall bias of the radar system. But, on some weather radars (e.g., WSR-88D) the antenna can not be pointed to 90°. A way to achieve absolute calibration in such cases has been devised by Ryzhkov et al. (2005). It uses dry aggregates at high elevation angles and claims accuracy better than 0.2 dB for the complete transmit-receive calibration of Z_{DR}. Hubbert et al. (2003) propose a sun scan through precipitation-free region to account for the receiving path, and cross-polar measurements from precipitation (or other scatterers) to account for the transmit path. The method is suited for radar that can measure all elements of the backscatter covariance matrix. Although sun scan is an excellent source for calibrating differential bias of the receiving path, it must be supplemented by calibration of the transmitting path (Hubbert et al. 2003; Zrnic et al. 2006). Moreover, because the effective antenna aperture size is proportional to the product of directivity and wavelength squared, a 3-cm wavelength radar has a disadvantage in sensitivity compared to a 10-cm wavelength radar of equal beamwidth. Therefore the solar flux at the 3-cm wavelength is marginally detectable and hence might not be suitable for monitoring calibration. Thus other viable alternatives are highly desirable.

Herein we exploit ground clutter differently than Sielberstein et al. (2008) to monitor stability of reflectivity and differential reflectivity and thus quantify temporal changes in bias. We consider polarimetric radars that operate by transmitting Simultaneously Horizontal and Vertical (SHV) polarization and likewise receive these. This mode is susceptible to variation in Z_{DR} imposed by changes in gains of the receivers (in horizontal and vertical channels).

2. EXPERIMENTAL SETUP AND DATA SET

We evaluate the stability of Z_H and Z_{DR} on data obtained from 21 November 2009 to 17 January

* *Corresponding author addr*ess: Dr. L. Borowska, NOAA's National Severe Storms Laboratory, Norman, OK, USA; e-mail: Lesya.Borowska@noaa.gov

2010 in Bonn, Germany and on three and one-half consecutive days (2-5 July, 2011) in Norman OK. The Bonn data contains 17 rainy days, 7 snow days, and 3 days with mixed snow and rain. It has been collected with a polarimetric X-band radar (BoXPol) belonging to the Meteorological Institute of the University of Bonn. The radar wavelength is 3.213 cm, peak power is 200 kW, pulse repetition time is 1 ms, and two-way pulse depth is 100 m. The 3-dB beamwidth (one-way) is 1.06° and the radar has no radome. BoXPol uses the SHV mode and records reflectivity factors at horizontal and vertical polarizations Z_H and Z_V, differential reflectivity Z_{DR}, differential phase Φ_{DP}, and correlation coefficient between horizontally and vertically polarized returns ρ_{HV}. These polarimetric variables are estimated using a long dwell time (90 contiguous time samples at a pulse repetition time of 1 ms).

The Oklahoma data were obtained with the WSR-88D (KOUN) recently upgraded to dual polarization by the National Weather Service. The radar operates in the SHV mode and has an automatic measurement and correction of differential reflectivity bias at end of each volume scan.

3. CLUTTER DETECTION

If the radar beams can be pointed at exactly the same azimuths from scan to scan (precise indexed beams) clutter map can be generated and used for locating strong ground clutter. We created a clutter map and made an attempt to use it, but found out that the detected positions varied slightly because of imperfect assignment of antenna pointing. Thus the map would need to encompass up to three degrees in azimuths to cover all possible shifts. Hence we settled for the much simpler detection based solely on the reflectivity and velocity thresholds.

We use measurements from 0.5° elevation angles and constrain the range to 20 km for Bonn data and to 7 km for Norman data. Clutter is strongest at close range and the effects of beam bending due to refractive index gradients are smaller at short distances (see section 4.2). Another advantage of close range is that a good portion of nearby clutter is from urban structures and therefore more likely has a very stable Z_H and Z_{DR}. In Bonn and Norman data precipitation was from light to moderate. There were no Z_H precipitation values larger than 49 dBZ. Therefore the simple threshold applied to reflectivity (Z_H>50 dBZ) was sufficient for detecting ground clutter.

We also examined the Doppler velocities from clutter in Bonn and found these to be at the smallest quantized levels next to zero (0.12 m s^{-1} or -0.12 m s^{-1}, hardware does not allow exact zero values). We added for X-band data the additional constraint that data passing the Z_H threshold must have velocities of 0.12 m s^{-1} or -0.12 m s^{-1}. In Norman data the Doppler velocity measurements were made on a separate scan from the scan for Z_H and Z_{DR}. The radials of the two scans were not precisely aligned. Therefore, the zero velocity from the Doppler scan was not suitable for discriminating clutter.

4. DATA ANALYSIS

First part of this section deals with analysis of data from the BoXPol. In the second section are the results obtained from the newly modified KOUN radar.

4.1 *Analysis of X-band radar data*

We start by examining the median values of Z_H, Z_V, Z_{DR} and the number M of the ground clutter detection plotted at 5 min increments for days with rain (Fig. 1). The median values of Z_{DR} contain a bias of -1.7 dB which has not been compensated because our interest here is in the trend and stability. From measurements at vertical incidence on Dec 10, 2009 we conclude that the correct clutter median value is -0.5 dB. Noteworthy is the stable and consistent median Z_H for rainy days (Fig. 1) and for snow days (not shown); we computed the standard deviation of the medians to be 0.09 dB for rainy days and 0.11 dB for days with snow. Quick look at the median Z_H and Z_V (Fig. 1) reveals their excellent stability. The majority of Z_H are 56 dBZ with a much smaller occurrence of 55.5 dBZ. As the quantization increment of the data is 0.5 dB we conclude that the true median is close to 56 dBZ and the variation of the radar system gain (H channel) and/or environmental conditions affecting strength of reflected signals is within the quantization interval. For most part the temporal change of the median Z_V (Fig. 1) is within 0.5 dB similar to the change of median Z_H (Fig. 1) except it exhibits faster fluctuation between the two quantized levels. This prompted a more detailed look at the characteristics of the data set. The number *M* of clutter detection varies within contiguous time

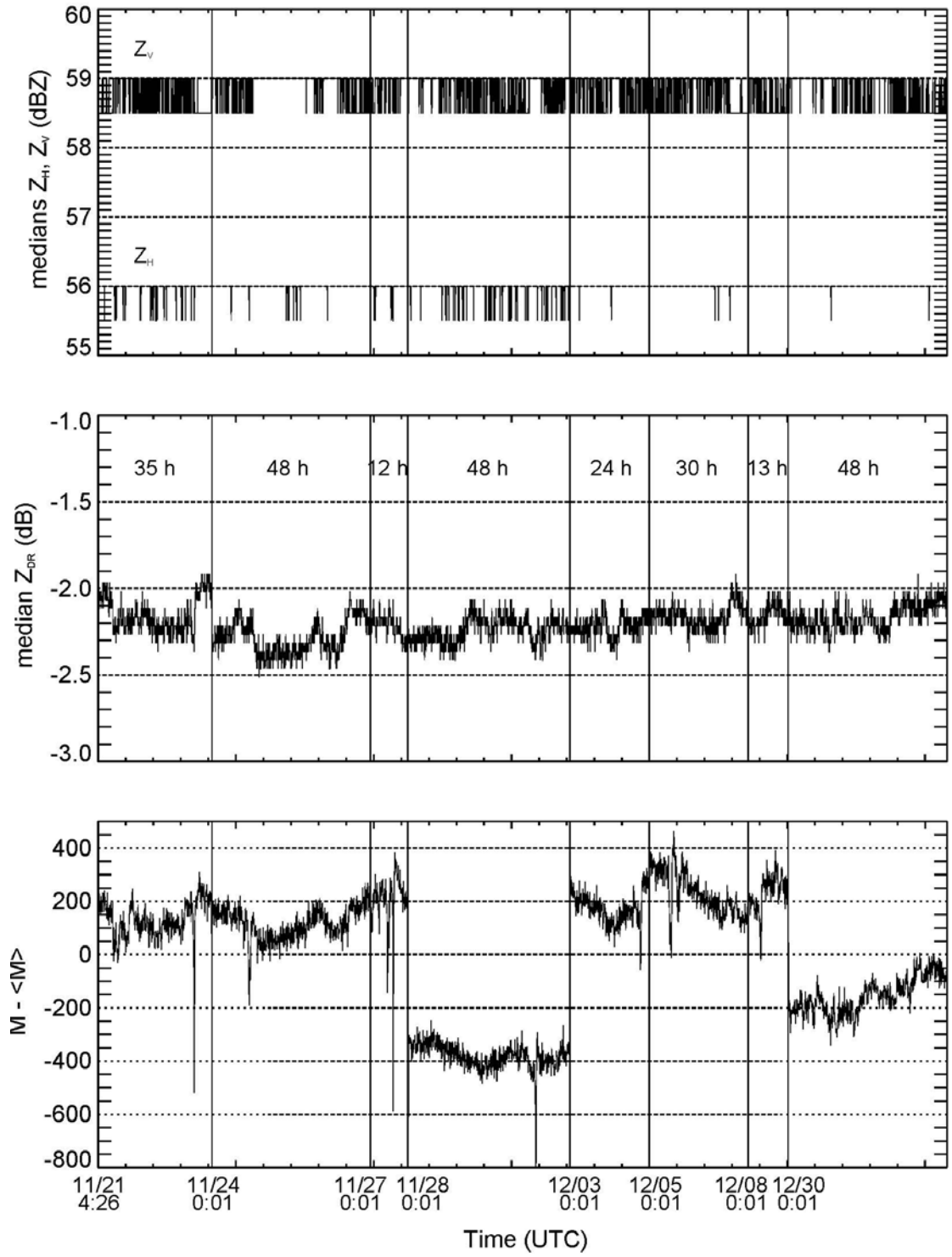

Fig. 1. Graph on top: medians of Z_H, Z_V from the ground clutter. Middle graph: same as on top except it is the median Z_{DR}. Bottom graph: difference between the total M and the average $\langle M \rangle$ = 4865 numbers of clutter detections. The thin vertical lines indicate temporal discontinuities between contiguous samples. The durations of the continuous measurements are written on the middle graph in hours and the beginning of each episode is indicated on the bottom graph in UTC. The thick marks on the time axis are in increments of 500 min.

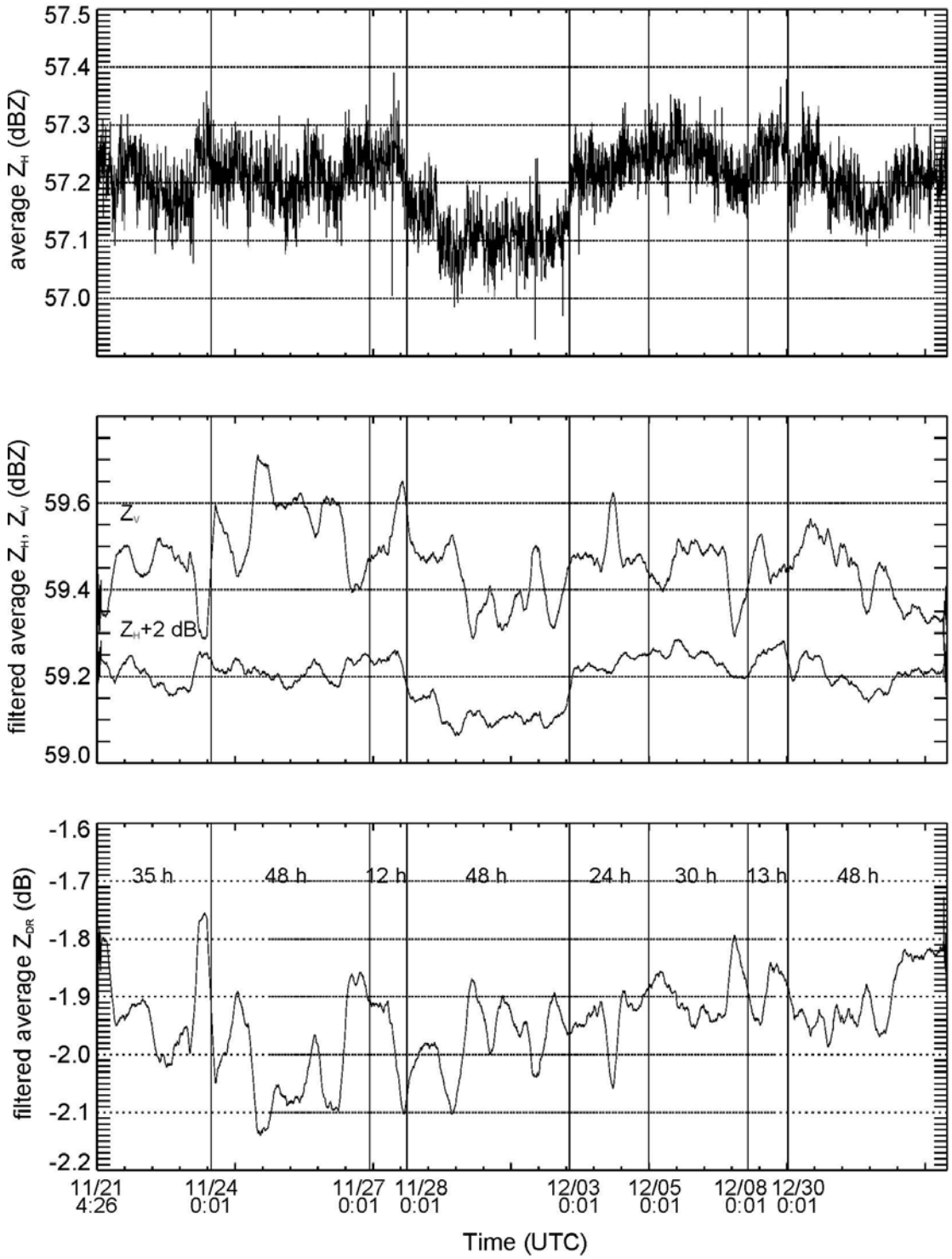

Fig. 2. Similar to Fig. 1 except: graph on top: average Z_H of ground clutter. Middle graph: thirty point running average of Z_H and Z_V; 2 dB is added to Z_H for visual clarity. Bottom graph: thirty point running average of Z_{DR}.

periods by less than 1.6% as can be seen in Fig. 1 where for visual clarity the difference $M - \langle M \rangle$ is plotted and $\langle M \rangle = 4865$ is the average for the whole span of data with rain. The vertical lines bracket uninterrupted data episodes and abrupt changes occur at each transition (i.e., coincide with the gaps in data). Largest steps (~ 10% to 15 % of the total number) occur on the 11/28, 12/03, and 12/30. These largest changes correlate with the decrease in the average values of clutter Z_H (Fig. 2 top and middle graphs) and Z_V (not shown) suggesting that a common cause influenced both channels. It could be a small systematic decrease (about 0.1 dB, Fig. 2) in transmitted power or some environmental factor. Thus we submit that the number of detections can serve a useful role in identifying times of the onset of change. Attribution of this change to a definite cause is difficult but the fact that such small change is detectable implies larger changes (~0.5 dB) should be easy to monitor.

The average values of Z_H (top Fig. 2) have definite trends not seen in the median due to coarse quantization. Superposed to the slower variations are rapid fluctuations suggestive of noise. To quantify and separate the two we analyzed the autocorrelations of averaged Z_H, Z_V, and Z_{DR}. This we did for each episode (separated by thin vertical lines in Fig. 1 and 2). The variances (i.e., signal) of Z_V are mostly four or more times larger than corresponding variances of Z_H. Also the SNRs of the Z_V are larger by a similar factor. The correlation coefficients (lag 0) between the average Z_H and Z_v are low with only three values exciding 0.5 suggesting that the environment is not a major cause of variations.

The changes in the noise variances (power in the jargon of electrical engineers) are within about ± 25 % of mean values which are 13×10^{-4}, 30×10^{-4}, and 16×10^{-4} dB^2 for the $\mathrm{Var}(Z_{HN})$, $\mathrm{Var}(Z_{VN})$, and $\mathrm{Var}(Z_{DRN})$; corresponding standard deviations are 0.036 dB, 0.055 dB and 0.04 dB. Data indicate correlation times of few hours hence we averaged over 2.5 hours (30 points) and plotted the values of filtered Z_H and Z_V in Fig. 4 (middle graph) and Z_{DR} in the bottom graph. Stability and consistency of filtered average Z_H is in contrast to the more variable Z_V which could be due to significant gain variations in the V chain. Otherwise the dominant influence of Z_V on Z_{DR} is quite visible as anti-correlation in the variations of the two. This is expected because the Z_V is linearly related to Z_{DR} (computation of Z_{DR} in the radar signal processor is from powers prior to conversion into reflectivities).

The results for the snow and mixed (snow and rain) cases are consistent with the rain episodes: the variability of Z_V is larger whereas that of Z_H is within 0.2 dB until the time when the number of samples M drops.

4.1 *Analysis of S-band radar data*

Just as in the case of X band the median Z_H from S-band data varies within the quantization interval (i.e., 53 dBZ and 53.5 dBZ) suggesting that monitoring of power calibration within 0.5 dB would be viable. The median Z_{DR} and the system Z_{DR}, defined as the measured bias, exhibit diurnal trend (Fig. 3). The same is very clearly seen in the average Z_H (Fig. 4). The surface temperature excursion on these three days was ~ 13^o C (Fig. 4) and the average Z_H from clutter has a minimum slightly lagging the time of maximum temperature. (The number of clutter detections has a similarly positioned minimum.) Because the boundary layer becomes well mixed after the time of maximum surface temperature the beam will be least bent at that time and hence would illuminate clutter with its lower values.

The autocorrelation coefficients of average Z_H and Z_{DR} (Fig. 5) show the diurnal periodicity and superposed higher frequency variations especially visible in the r_{ZH} plot. The high frequency variations have a period of approximately 50 min and are caused by periodic variation of the antenna elevation angle (Fig. 5, bottom). Examination of the scanning process (recorded in the data) reveals that every volume scan begins at an azimuth angle on the average 66^o larger than the previous one (the position varies randomly between 60^o and 75^o). Thus at the end of the fifth scan the antenna is positioned ~ 30^o behind in azimuth from the first scan. For other scans relatively close to the batch of five the starting position of the antenna is further away from the first scan. This basic periodicity of five is highly correlated with the antenna elevation variations which are within 0.04^o of the mean (not shown). Such small variations cause less than 0.1 dB change (not shown) in the Z_H. The change in elevation with the starting azimuths of volume scans might be coincidental; some other factor such as periodic drift in the servo control might have caused it. We add that the KOUN pedestal is one of a kind (it is the pre-production model of the WSR-88D). Hence we do not know if a similar effect is

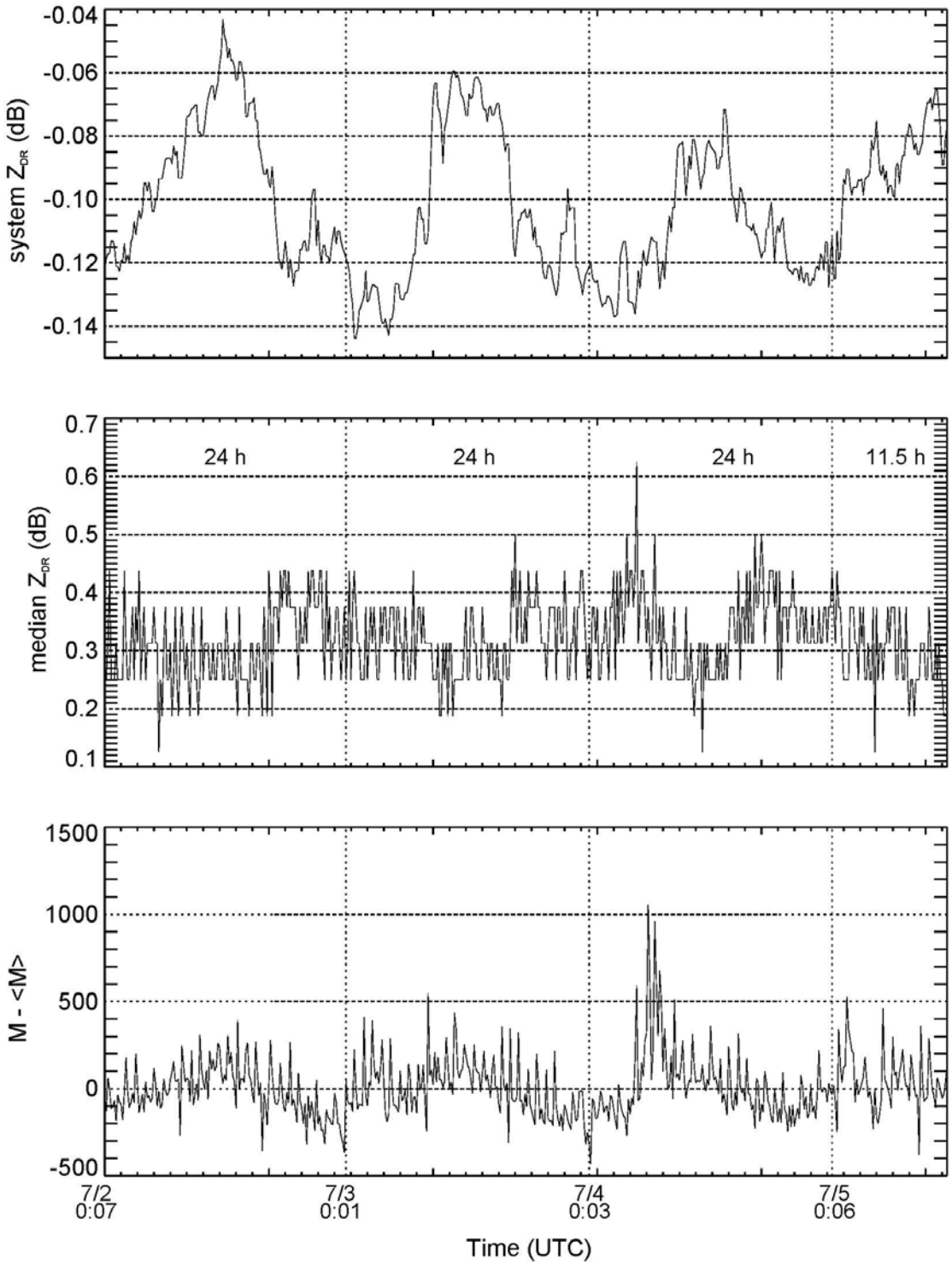

Fig. 3. Top graph: system Z_{DR} obtained automatically at end of volume scans using signal generator and a prior initial calibration. Dotted vertical lines indicate beginning of a day (UTC time); the dates and minutes of the beginning are indicated along the abscissa. Middle graph: median Z_{DR}. Bottom graph: the difference between the number of points M and its average value (<M>=2742). Data obtained with the pre-production model of the WSR-88D. The thick mark on the abscissa corresponds to ten consecutive volume scan (accomplished in 9.73 min).

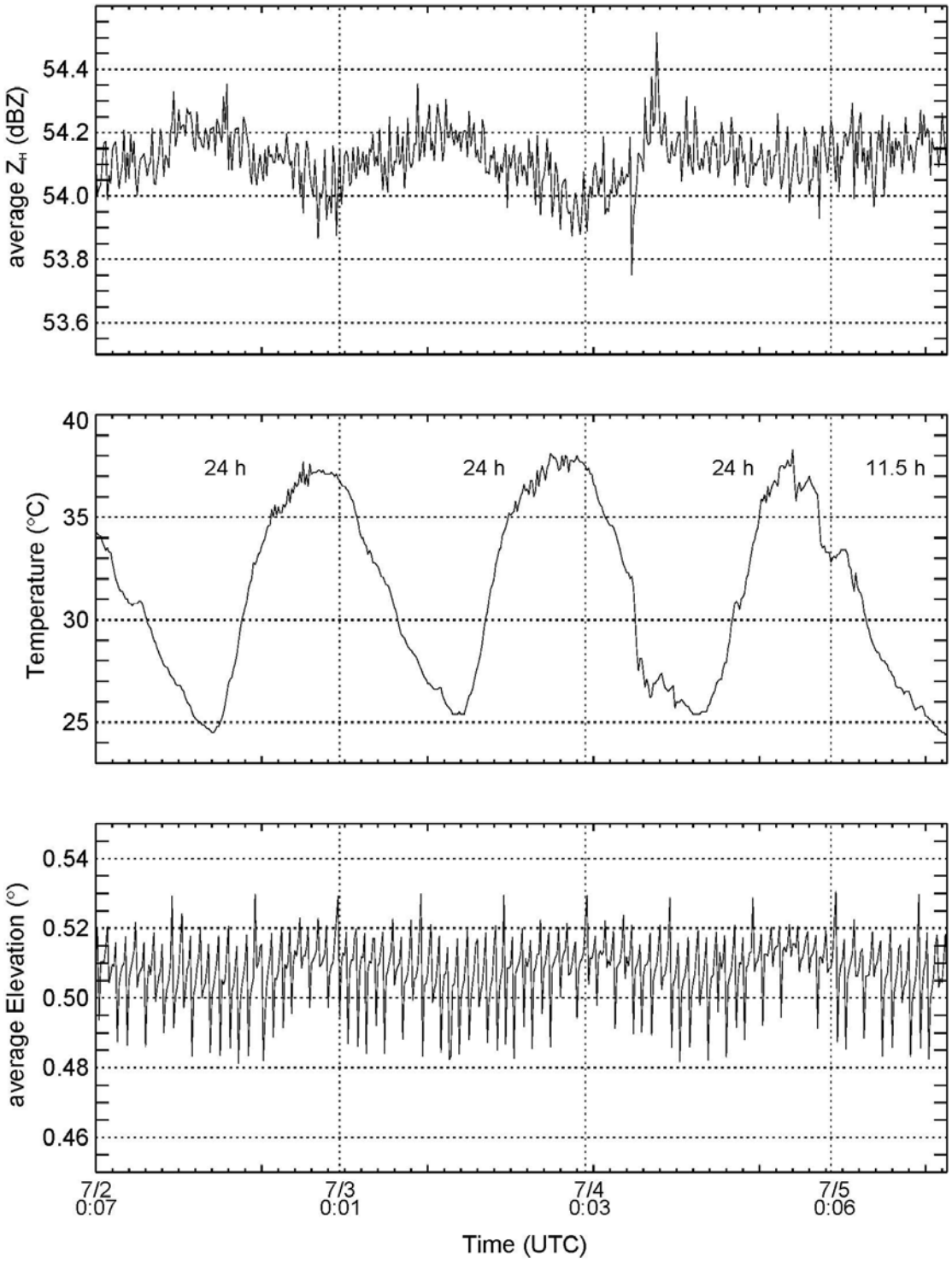

Fig. 4. Top graph: average Z_H from clutter. Middle graph: surface temperature. Bottom graph: average elevation angle of the lowest (commended to be 0.5^o) scan. Times and thick marks are as in Fig. 3.

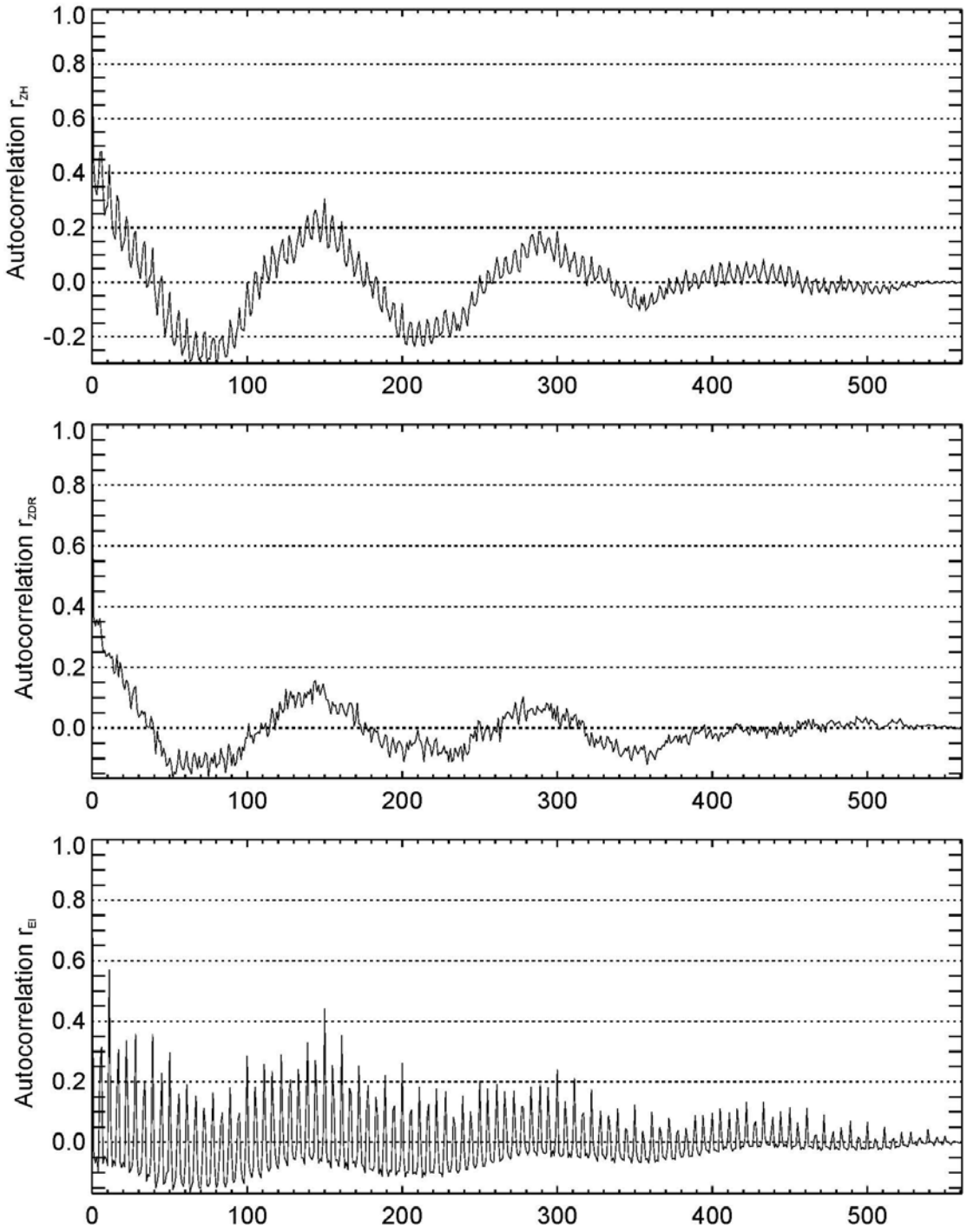

Fig. 5. Top graph: autocorrelation coefficient of Z_H. Middle graph: autocorrelation coefficient of Z_{DR}. Bottom graph: autocorrelation coefficient of average elevation angle. The thick marks are at lag 10 corresponding to ten scans separated by 9.73 min. The linear tapers with lag are caused by the linear decrease in the number of points normalized to the total number of points in computation of the autocorrelations.

present on other WSR-88Ds as these have larger and more robust units.

Next we concentrate on the time ~ 4 to 7 UTC, July 4, when the number of detections increased significantly (500 to 1000 more). The increase is by a factor of two (from ~ 6000 to ~ 12000) if clutter up to 20 km in range is included. We examined the data and found that a storm moved over the radar at 4:00 UTC and stalled. At 5:00 it begun to dissipate rapidly, extinguished by precipitation embedded in a downdraft. The ensuing cool air (see the sharp temperature drop after ~ 2.5 UTC, Fig. 4) spread and created an inversion conducive to beam bending toward ground hence the increase in the number of detections (Fig. 3 bottom) and average Z_H (Fig. 4, top). Note that the increase in median Z_{DR} (Fig. 3 middle) precedes the increase in Z_H, likely due to wetness as opposed to contamination by precipitation as there is no increase in the number of detected points. The rain came after many days of extremely hot dry weather hence it could have influenced clutter reflectivity.

5. DISCUSSION

Analysis of data suggests that the average of ground clutter reflectivities is sufficiently stable over a month's period in a cool environment (Germany) that it can be used to monitor radar calibration. In three and one-half days of hot summer environment in Oklahoma the reflectivities of clutter were similarly stable. Combined with the number of detections measurements of clutter Z_H can point to changes which affect calibration. Following is a list of influences on measurements of Z and Z_{DR} from clutter:

1) changes in transmitted power;
2) changes in receiver transfer function (mainly gains);
3) antenna settling in elevation from scan to scan;
4) differences in beam pointing (azimuth) at subsequent scans;
5) variation of clutter reflection coefficient;
6) refraction of the beam;
7) changes in attenuation due to precipitation.

Some of the changes can be isolated and related to radar problems but for monitoring calibration the changes in transmitted power and receiver transfer function need to be quantified. Influence of transmitted power variation on Z calibration is resolved with direct power measurements. On occasions there can be other impediments such as accumulation of snow on the radome; monitoring of ground clutter can alert engineers about these. One can set a threshold (say 0.5 dB) and take action if the threshold is exceeded. If one of the Zs from clutter stays constant (say within 0.1 dB) as Z_H in Fig. 1 (within each episode) but the other exhibits variations suggests the transmitter power is stable and the likely cause is in the receiving chain and a correction to Z_{DR} bias would be warranted. If both reflectivities exhibit significant correlated variations would suggest a common cause such as transmitted power change or environmental influence.

Consider antenna settling at slightly different elevations from scan to scan. For Bonn data the mid range of clutter contribution is 10 km and if 0.05^o variation in elevation occurs there would be a corresponding vertical displacement of the beam by 8.7 m. The extent of the main lobe from center to the null is more than 1^o. Therefore at 0.5^o elevation the principal contribution of clutter is through the steep part of the main lobe. Further the change in antenna pattern value over a 0.05^o (at 1^o off axis) is 2.5 dB. Clearly this large variation would be seen in the plots of Z_H or Z_V. The fact that it is not seen implies the variations are much smaller or not present. We would expect these to be random but not systematic as observed in Fig. 1 (average Z_H, Z_V).

In data from the polarized KOUN (pre-production WSR-88D) the variations in elevation (0.04^o peak to peak) are periodic and correlate with the corresponding variations (0.2 dB peak to peak) in Z_H from clutter. These are due to the azimuthal dependence of antenna settling at the beginning of volume scans. Although very small the variations are easily detected because of the large number (few thousand) of ground clutter points.

If the main lobes for the H and V polarizations differ slightly in width, the Z_H and Z_V would be positively correlated. If antenna position changes (up or down) then both reflectivities would decrease if antenna has moved up and increase if down. Z_{DR} would increase if antenna moves up and the H pattern is wider (larger than the V pattern at the same distance from beam axis) because the difference of patterns at places the beam hits ground increases. If the H pattern is narrower then the Z_{DR} will decrease. On the KOUN radar the changes in elevation and Z_{DR} are out of phase indicating that the beamwidth at V polarization is broader than at H polarization by about 0.04^o.

Imperfect beam positioning in azimuth can also cause variation in Zs and Z_{DR} from scan to scan. The effect is similar to the one from beam settling in elevation and it might have a periodic component. Briefly the exact position in azimuth is not in perfect sync with the timing of samples for computing estimates of polarimetric variables. Thus, the position of the beam at the center of dwell time differs from scan to scan. The value of Z_H and Z_V would be affected just the same as in case of settling in elevation. An increase in both occurs if in the subsequent scan the effective beam center is pointing closer to the dominant ground scatterer. Otherwise a decrease in both follows. The differential reflectivity would be influenced by the difference in azimuthal beamwidths just as it is in case of elevation changes.

We do have evidence of change in effective pointing direction of the antenna on the BoXPol which manifested itself in a smaller number of clutter detections due to decrease in the reflectivities. Also occasional changes in range location were noted.

Short term changes in the reflection coefficient from urban clutter can be caused by wetness. We expect these to be similar for Z_H and Z_V hence the two would be highly correlated and perhaps not affect Z_{DR}. But we have circumstantial evidence that wetness after a dry period in Oklahoma might be a reason for increased Z_{DR}; the clutter environment in Norman is a mix of suburban houses and open rolling prairie with small trees which might make a difference. Long term changes (due to presence or absence of leaves on trees) might also affect Z_{DR}.

Banding of the beam due to change in the profile of refraction can have a significant influence on Zs and Z_{DR}. In the cool regime like winter in Bonn no diurnal trend are evident as the refraction profile changes little throughout the day. Nonetheless, a change due to passage of cold front correlates well with the increase in the number of detections and average values of Z_H, and Z_{DR}. Diurnal periodicity is evident in the data from Oklahoma and is highly correlated with the surface temperature. Moreover, an episode of cool outflow from a dissipating storm cell created a stable layer which caused significant beam bending and increase in Z_H. Although small (few tenths of a dB) the changes are very well defined.

Change due to attenuation can be significant and in heavy precipitation would preclude calibration of Z and Z_{DR} from clutter returns. Perhaps the amount of attenuation could be diagnosed and cautiously used for corrections of reflectivities and differential reflectivities caused by these effects. But systematic correction of biases by drifts in hardware would be very difficult in case of heavy precipitation. Still ground clutter returns between episodes of heavy precipitation might suffice to monitor the radar status.

6. REFERENCES

Borowska, L., D. Zrnic, A. Ryzhkov, P. Zhang, and C. Simmer, 2010: Long term measurements of rain in the cold season with a 3-cm wave length polarimetric radar. *J. Hydrometeor*. (accepted).

Bringi, V. N., and V. Chandrasekar, 2001: *Polarimetric Doppler Weather Radar.* Cambridge University Press, 636 pp.

Edelson, S., 1962: Calculations of a slowly varying component at 4.3 mm. *Astrophys. J.*, **135,** 827-833.

Gorgucci, E., G. Scarchilli, and V. Chandrasekar, 1999: A procedure to calibrate multiparameter weather radar data using the properties of the rain medium. *IEEE Trans. Geosci. Remote Sens.,* **17,** 269–276.

Hubbert, J.C., M. Dixon, S. Ellis, G. Meymaris, 2009: Weather Radar Ground Clutter, Part I: Identification, Modeling and Simulation. *J. Atmos. Oceanic Technol*., **26,** 1165-1180.

Rinehart, R. E., 1978: On the Use of Ground Return Targets for Radar Reflectivity Factor Calibration Checks. *J. Appl. Meteor.,* **17,** 1342–1350.

Ryzhkov, A., S. Giangrande, V. Melnikov, and T. Schuur, 2005: Calibration issues of dual-polarization radar measurements. *J. Atmos. Oceanic Technol*., **22,** 1138–1154.

Silbertstein, D. S., D. B.Wolff, D.A. Marks, D. Atlas, and J.L. Pippitt, 2008: Ground clutter as a monitor of radar stability ad Kwajalein, RMI. *J. Atmos. Oceanic Technol*. **25,** 2037-2045.

Zrnic, D.S., V.M. Melnikov, and J.K. Carter, 2006: Calibrating differential reflectivity on the WSR-88D. *J. Atmos. Oceanic Technol*., **23,** 944-951.